Using Numerical Weather Prediction Model Derived Tropospheric Slant Delays in GPS Processing: a Case Study

Maaria Nordman[1], Reima Eresmaa[2], Markku Poutanen[1], Heikki Järvinen[2], Hannu Koivula[1] and Juha-Pekka Luntama[2]

[1] Finnish Geodetic Institute, P.O.Box 15, 02431 Masala, Finland
[2] Finnish Meteorological Institute, P.O.Box 503, 00101 Helsinki, Finland

Abstract

The troposphere is one of the most significant sources of error in precise GPS (Global Positioning System) positioning solutions nowadays. Uncertainties in troposphere estimation distort the height component especially. We have implemented the troposphere slant delays derived from a numerical weather prediction model to GPS processing. In this case study we calculated 24 vectors for 61 days, the length of the vectors varying between 110 and 1100 km. When the slant delay is used instead of a standard troposphere model the variation in the positions solution's up component is reduced considerably. At Sodankylä station (67.42ºN, 26.39ºE), for example, the standard deviation decreases from 5.9 cm to 1.3 cm for this 61-day period if no site-specific troposphere parameters are estimated. We also found that the length of the vector did not greatly affect the variance in the slant delay based positioning solutions.

Key words: global positioning system (GPS), tropospheric delay, numerical weather model (NWM)

1. Introduction

Different satellite geodetic techniques based on microwave frequencies are used widely and the demands concerning their accuracy are increasing. One of the problems restricting this accuracy is the estimation of the tropospheric delay. The effect is hard to compute with an adequate spatial and temporal resolution. A traditional mapping function approach includes two parts, firstly the a priori zenith delay and secondly the elevation angle dependence of the delay. In general, the zenith delay is related to the slant delay by a mapping function.

Today, several mapping functions have been developed and are widely used. The Niell mapping function (NMF) (*Niell,* 1996) is based on climatological temperature and relative humidity profiles and is independent of the surface meteorology. The next-generation mapping functions are based on numerical weather models (NWM). They include e.g. the isobaric mapping function (IMF) (*Niell,* 2001) and the Vienna mapping function (VMF) (*Boehm and Schuh,* 2004) and the VMF1, an improved version of the

latter (*Boehm et al.,* 2006a). The IMF uses intermediate parameters of NWM whereas the VMF and VMF1 parameters are based on ray tracing through the atmosphere. Global mapping function (GMF) was developed to combine the accuracy of VMF1 and the coverage of NMF (*Boehm et al.*, 2006b). A comparison of the performance of these mapping functions for VLBI (Very Long Baseline Interferometry) analysis can be found in *Tesmer et al.* (2007).

Different techniques such as radiosonde, water vapour radiometers, GPS and VLBI, have been used for troposphere delay validation (*Niell et al.* 2001; *Snajdrova et al.* 2006 and references therein). Studies have also been made of using GPS and VLBI for water vapor estimation and input for weather models, e.g. *Vedel et al.* (2004) and *Troller et al.* (2006).

Sophisticated GPS processing software uses various troposphere models and mapping functions. New and more accurate models are continuously under development but they are mostly available only for scientific software. Most of the mapping functions depend solely on the elevation angle and are therefore insensitive when, for instance, a synoptic disturbance passes over, meaning that the delay also changes with the azimuth.

We present a method for utilizing NWM-based troposphere delays, which are both azimuth and elevation angle dependent, on the observation level. Corrections on the observational level can also be applied for other error sources. *Tregoning and van Dam* (2005) used a similar approach for correction because of crustal loading.

We have used a double difference solution of the Bernese v. 5.0 (*Dach et al.* 2007) to compute a vector between two stations. One station is kept fixed and the coordinates of the other station are estimated with and without site-specific troposphere parameter estimation. We have used two months of data for our case study in order to compare the performance of the widely used mapping function based approach to the direct ray tracing approach of tropospheric correction. These are the first results and we concentrate here on the up component of the solution because it is the most sensitive to the troposphere. An accurate up component time series could be used for several geophysical studies, e.g. various loading studies.

2.   *Derivation of the slant delay from the NWM*

Tropospheric slant delay is determined by using numerically forecasted values of pressure (p), temperature (T) and specific humidity (q) in a three-dimensional grid. These forecast fields are produced by the High Resolution Limited Area Model (HIRLAM). HIRLAM (*Undén et al.* 2002) is developed and maintained by nine national meteorological institutes in Europe, and its output is utilized operationally in daily weather forecasting. The lateral boundary conditions for HIRLAM are retrieved from the global forecasts of the European Centre for Medium-Range Weather Forecasts (ECMWF). The initial condition (analysis) for the forecast is obtained through the variational data assimilation process (*Gustafsson et al.* 2001; *Lindskog et al.*, 2001). A

report has also been published on use of the HIRLAM for mapping function coefficient determination (*Stoyanov et al.* 2004).

Slant delay is obtained through numerical integration of the refractivity N along the signal path s, in accordance with the commonly used definition for tropospheric re-fraction Δ^T

$$\Delta^T = \int_s (n-1)ds = 10^{-6} \int_s Nds \qquad (1)$$

As shown by *Eresmaa and Järvinen* (2006), N depends on the HIRLAM model variables through

$$N = \frac{k_1 p}{T} + \frac{(k_2 - k_1)qp}{(0.622 + 0.378q)T} + \frac{k_3 qp}{(0.622 + 0.378q)T^2} \qquad (2)$$

under the ideal gas assumption. We used values $k_1 = 77.60$ K hPa^{-1}, $k_2 = 70.4$ K hPa^{-1} and $k_3 = 3.739 \times 10^{-5}$ K^2 hPa^{-1} for the refractivity coefficients in (2), as suggested in *Bevis et al.* (1994).

Slant delay is a function of the elevation and the azimuth of the satellite, in addition to the receiver coordinates and time epoch. The signal path determination relies on the layer-wise approximation of a straight geometric line across the HIRLAM grid. In order to account for the refractive bending, an explicit correction, based on the refractivity profile, is applied on top of the straight-line approximation on each. The algorithm is described in more detail by *Eresmaa and Järvinen* (2006).

This study applies the HIRLAM model with a horizontal grid spacing of 9 km on 40 layers. For each GPS observation epoch, the numerical forecast with the shortest possible lead-time is used. Since HIRLAM analyses are produced every six hours and the model output is recorded for every forecast hour, the slant delays are determined using forecasts with lead times between 0 and 5 hours.

3.   GPS processing

We used the slant delays produced from the HIRLAM and interpolated them for every five minutes in the direction of each satellite. From these we computed the delays for every observation epoch using linear interpolation. The effect of the troposphere in the GPS observables was removed by correcting the observed code and carrier pseudo-ranges with the slant delays. Corrections were made on the observational level directly in the standard RINEX (Receiver Independent Exchange Format) files for each satellite and each epoch before processing. This allows us to use the slant delay approach with any software that has the option of switching off the troposphere estimation. Hereafter this method is referred as HSD (Hirlam Slant Delay).

We used data from the Finnish permanent GPS network, Finnref. The network consists of 13 stations between the latitudes 60° and 70° N (Fig. 1). The lengths of the vectors and the amount of data used for each vector are shown in Table 1. A total of 61

days of data from 16 September to 15 November 2005 were used. The period was chosen because several synoptic disturbances were passing over Finland then, so we expected major changes in the tropospheric delay.
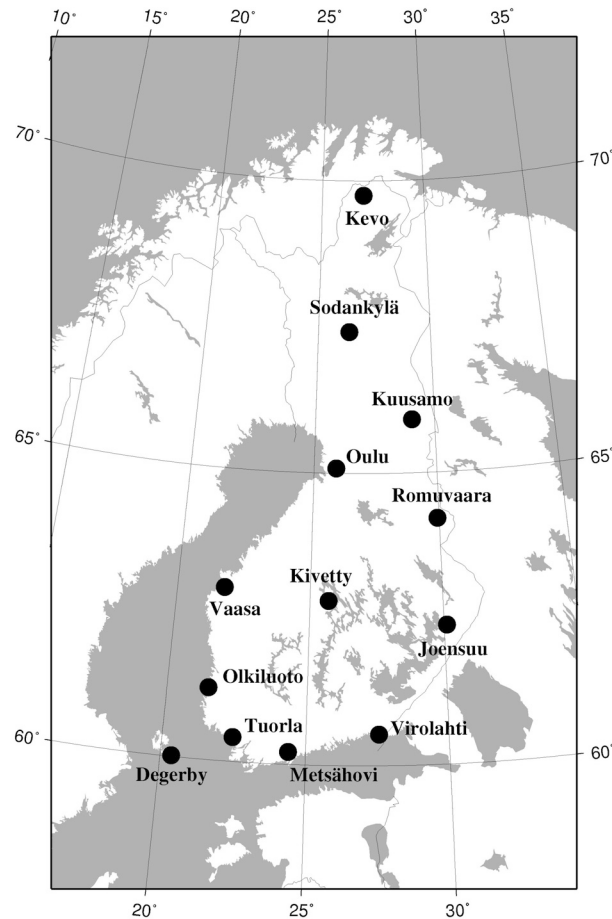

Fig. 1. The Finnref stations.

The computations were carried out using the Bernese v. 5.0 software (*Dach et al.* 2007) for the ionosphere-free L3 combination in double difference mode. We calculated a total of 24 vectors, twelve keeping Metsähovi fixed and twelve more keeping Oulu fixed. The length of the vectors varies from 110 km to 1100 km (see Table 1). The elevation cut-off angle was set at 5° and the elevation-dependent weighting was adopted. We calculated all the time series in the same way except for the troposphere handling. There were four different processing schemes used for the troposphere:

(1)   using the NMF

(2)   using the HSD

(3)   using the NMF as a priori and estimating the site-specific troposphere parameters

(4)   sing the HSD as a priori and estimating the site-specific parameters.

In scheme (1) Saastamoinen zenith delays are used with the Niell mapping function and the scheme (2) uses the HSD described above. These two schemes

simulate the use of a non-scientific processing software. In the processing program used here (Bernese) it is possible to estimate site-specific parameters to gain more accurate results. These site-specific parameters used in (3) and (4) are station and time dependent corrections to the a priori model. We have used the wet NMF for the parameter estimation with parameter spacing of four hours. In this case study horizontal gradients were not estimated.

Table 1. Names and lengths of the vectors and number of days used in the analysis. DE = Degerby, JO = Joensuu, KE = Kevo, KI = Kivetty, KU = Kuusamo, ME = Metsähovi, OU = Oulu, OL = Olkiluoto, RO = Romuvaara, SO = Sodankylä, TU = Tuorla, VA = Vaasa, VI = Virolahti.

Vector	L - km	Days	Vector	L - km	Days
METU	110	61	MEJO	390	61
OUKU	175	60	OUOL	485	61
MEVI	180	61	OUVI	515	61
MEOL	195	61	OUKE	525	61
OURO	215	46	MERO	530	46
MEDE	225	49	MEOU	545	61
OUKI	250	61	OUME	545	61
OUSO	260	61	OUTU	550	61
MEKI	300	61	OUDE	630	49
OUVA	310	61	MEKU	675	60
MEVA	335	61	MESO	810	61
OUJO	365	61	MEKE	1070	61

4.   Results and discussion

The up component time series for all the processing schemes for the Sodankylä station are plotted in Figure 2. The vectors calculated are Metsähovi–Sodankylä (MESO, length 810 km, circles) and Oulu–Sodankylä (OUSO, length 260 km, crosses). The standard deviation of the scheme (1), being 5.9 cm, improved 79 % when scheme (2) was used. This improvement is achievable for any processing software that allows the troposphere modelling to be switched off. Schemes (3) and (4) gave almost similar results with a sub-centimetre standard deviation and a 10% improvement from scheme (3) to scheme (4).

The standard deviations of the up component time series for all the vectors are shown in Figure 3 as a function of the vector length. The standard deviations were calculated after outlier removal. Figure 3a depicts the solutions for schemes (1) and (2). The distance dependence is 84 ppm when the NMF is used in the solution and 3 ppm when the HSD is used. The reduction in standard deviation is 78% for all the vectors. Figure 3b presents the difference between processing schemes (2), (3) and (4). The solutions where site-specific parameters were estimated show smaller standard

deviations than the solution using slant delay alone. The difference between processing schemes (3) and (4) is small, and using the HSD results in only 3% smaller standard deviations on average.
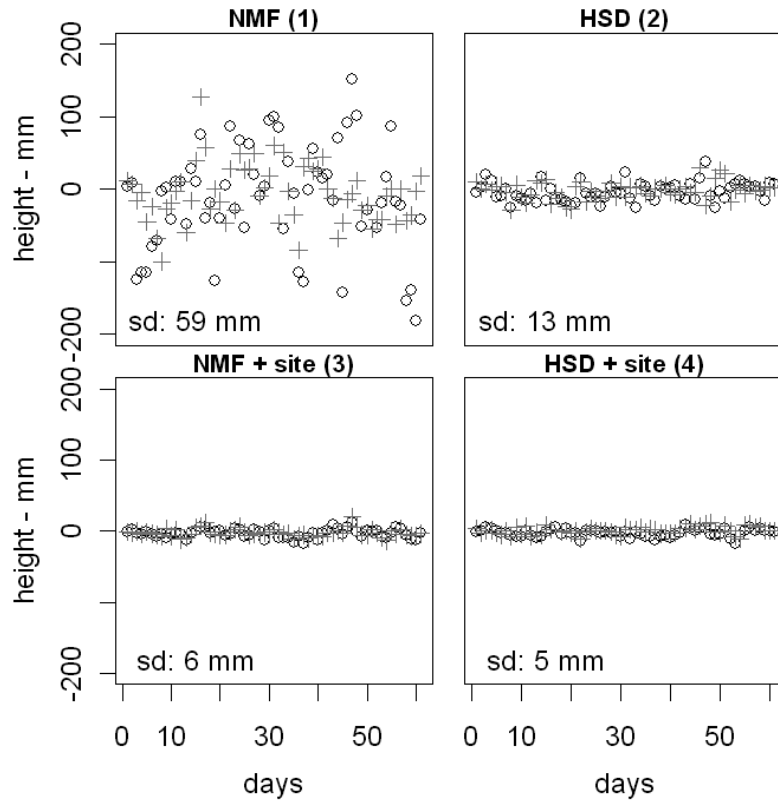

Fig. 2. The up component of the Sodankylä station. The left column indicates the solutions using the NMF and the right column the solutions using the HSD. The top row indicates the solutions without the site-specific parameters and on the bottom row the solutions with the parameters. The circles are the time series for vector MESO (810 km) and the crosses the vector OUSO (260 km). The standard deviations for each time series are plotted on the lower left corner. All the figures have the same scale.
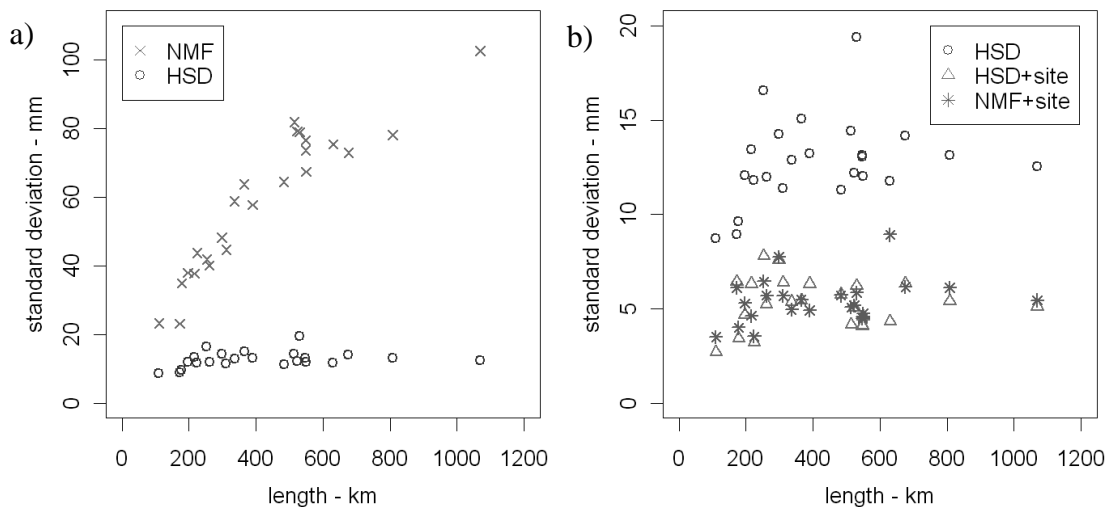

Fig. 3. Standard deviations of the up component time series relative to the length of the vector. The time series were produced using processing schemes (1) and (2) in a) and schemes (2), (3) and (4) in b).

Moreover, the solutions are very site-dependent, which can be explained by other errors dependent on satellite elevation, such as multipath. These errors are also evaluated if the site-specific troposphere parameter is estimated. For the Sodankylä station, for example, the HSD is 10% better whereas for the Vaasa station the NMF solution is 10 % better.

The reductions in the standard deviation for the GPS time series are quite drastic, as Figures 2 and 3 show. The performance of commonly used mapping functions is known to be of poorer quality at higher latitudes. All our stations are between the latitudes 60° N and 70° N. Because the GPS satellite constellation is not optimal, the satellites are seen at low elevation angles and the tropospheric delay may deviate considerably from the standard model value. Slant delays derived from the HIRLAM are also azimuth-dependent, taking into account synoptic disturbances passing over Finland. In the results passing synoptic disturbances could not be seen, this is probably due to the 24-hour processing window.

The difference between the schemes (3) and (4) is quite small in most cases. However, there are some advantages of the technique described here. Slant delay approach can be applied on any software capable switching off the troposphere estimation whereas site-specific option is available in some scientific software only. We can also add the effect of any other phenomena in the same way including ionosphere and loading. In the site-specific estimation we can not separate the troposphere correction because other elevation dependent phenomena (like multipath) are also convolved in results. If we could separate and model site-specific errors we could have a stronger and more accurate GPS positioning solution with less unknown parameters and shorter time series. The disadvantage of the slant delay method is that it requires an access to the HIRLAM.

5.   *Conclusions and outlook*

In this work we have used a method in which ground-based slant delays derived from a numerical weather model are directly subtracted from the GPS observables. These observations can then be processed using any GPS software that has the option of switching off the troposphere modelling. We used two months of data from autumn 2005 to compare the slant delay approach to the standard troposphere model.

We have shown that using the HSD improves the repeatability of the GPS solution. For all vectors, the reduction in the standard deviation is 78% in the up component in comparison of the NMF and the slant delay calculations. When the site-specific troposphere parameters are estimated, the reduction is not statistically significant. The slant delay model is also less sensitive to the length of the vector than standard models (e.g. Niell, Saastamoinen).

We presented the first results from the case study containing only 2 months of data. The project continues with processing longer time series. We will include the gradient estimation and study the influence of the HSD model on horizontal coordinates as well. We have also preparations on the way for using other zenith delay models as

well as other mapping functions, comparisons in this study were done to see the difference between the HSD and a basic mapping function approach.

Acknowledgements

References

Bevis, M., S. Businger, S. Chiswell, T. A. Herring, R. A. Anthes, C. Rocken, and R H Ware, 1994. GPS meteorology: Mapping zenith wet delays onto precipitable water. *J. Appl. Meteor., 33,* 379–386.

Boehm, J. and H. Schuh, 2004. Vienna mapping functions in VLBI analyses. *Geophys. Res. Lett., 31*:L01603, doi:10.1029/2003GL018984.

Boehm, J., B. Werl, and H. Schuh, 2006a. Troposphere mapping functions for GPS and very long baseline interferometry from European Centre for Medium-Range Weather Forecasts operational analysis data, *J. Geophys. Res., 111*, B02406, doi:10.1029/2005JB003629.

Boehm J., A. Niell, P. Tregoning and H. Schuh, 2006b. Global Mapping Function (GMF): A new empirical mapping function based on numerical weather model data, *Geophys. Res. Lett., 33,* L07304, doi:10.1029/2005GL025546.

Dach, R., U. Hugentobler, P. Fridez and M. Meindl (Eds.), 2007. *Bernese GPS Software, Version 5.0,* 612 pp., Astronomical Institute, University of Berne.

Eresmaa, R and H Järvinen, 2006. An observation operator for ground-based GPS slant delays, *Tellus, 58A,* 131–140.

Gustafsson, N., L. Berre, S. Hörnquist, X.-Y. Huang, M. Lindskog, B. Navascués, K. S. Mogensen, and S. Thorsteinsson, 2001. Three-dimensional variational data assimilation for a limited area model. Part I: General formulation and the background error constraint. *Tellus, 53A,* 425–446.

Lindskog, M., N. Gustafsson, B. Navascués, K. S. Mogensen, X.-Y. Huang, X. Yang, U. Andræ, L. Berre, S. Thorsteinsson and J. Rantakokko, 2001. Three-dimensional variational data assimilation for a limited area model. Part II: Observation handling and assimilation experiments. *Tellus, 53A,* 447–468.

Niell, A. E., 1996. Global mapping functions for the atmosphere delay at radio wavelengths. *J. Geophys. Res., 101*(B2), 3227–3246.

Niell, A. E., 2001. Preliminary evaluation of atmospheric mapping functions based on numerical weather models, *Physics and Chemistry of the Earth, 26,* 475–480.

Niell A. E., A. J. Coster, F. S. Solheim, V. B. Mendes, P. C. Toor, R. B. Langley and C. A. Upham, 2001. Comparison of measurements of atmospheric wet delay by radiosonde, water vapor radiometer, GPS, and VLBI. .*J. Atmos. Oceanic Technol., 18*, 830–850.

Snajdrova, K., J. Boehm, P.Willis, R. Haas and H. Schuh, 2006. Multi-technique comparison of tropospheric zenith delays derived during the CONT02 campaign, *J. Geod.,* **79**, 613–623, doi 10.1007/s00190-005-0010-z.

Stoyanov, B., R. Haas and L. Gradinarsky, 2004. Calculating Mapping Functions from the HIRLAM Numerical Weather Prediction Model, in *International VLBI Service for Geodesy and Astrometry 2004 General Meeting Proceedings,* edited by N.R. Vandenberg and K.D. Baver, p. 471–475, NASA/CP-2004-212255.

Tesmer, V., J. Boehm, R. Heinkelmann and H. Schuh, 2007. Effect of different tropospheric mapping functions on the TRF, CRF and position time-series estimated from VLBI, *Journal of Geodesy,* doi:10.1007/s00190-006-0126-9.

Tregoning, P. and T. van Dam, 2005. Atmospheric pressure loading corrections applied to GPS data at the observation level, *Geophys. Res. Lett.*, **32**, L22310, doi:10.1029/2005GL024104.

Troller, M., A. Geiger, E. Brockmann and H.-G. Kahle, 2006. Determination of the spatial and temporal variation of tropospheric water vapour using CGPS networks, *Geophysical Journal International,* **167**, 509–520, doi:10.1111/j.1365-246X.2006.03101.x.

Undén, P., L. Rontu, H. Järvinen, P. Lynch, J. Calvo, G. Cats, J. Cuxart, K. Eerola, C. Fortelius, J. A. Garcia-Moya, C. Jones, G. Lenderlink, A. McDonald, R. McGrath, B. Navascués, N. Woetman Nielsen, V. Ødegaard, E. Rodriguez, M. Rummukainen, R. Rõõm, K. Sattler, B. Hansen Sass, H. Savijärvi, B. Wichers Schreur, R. Sigg, H. The and A. Tijm, 2002. *HIRLAM-5 Scientific Documentation*, Available from Hirlam-5 Project, c/o Per Undén, SMHI, S-60176, Norrköping, Sweden. 144 pp.

Vedel, H., X.-Y. Huang, J. Haase, M. Ge, and E. Calais, 2004. Impact of GPS Zenith Tropospheric Delay data on precipitation forecasts in Mediterranean France and Spain, *Geophys. Res. Lett.,* **31**, L02102, doi:10.1029/2003GL017715.